Iranian Journal of Geophysics, Vol. 9, N0. 5, 2016, Page 40-56

A simple form of MT impedance tensor analysis to simplify its decomposition to remove the effects of near surface small-scale 3-D conductivity structures

Ali Moradzadeh

Professor, School of Mining, College of Engineering, University of Tehran, Tehran, Iran

(Received: 07 May 2014, accepted: 31 May 2015)

Abstract

Magnetotelluric (MT) is a natural electromagnetic (EM) technique which is used for geothermal, petroleum, geotechnical, groundwater and mineral exploration. MT is also routinely used for mapping of deep subsurface structures. In this method, the measured regional complex impedance tensor (Z) is substantially distorted by any topographical feature or small-scale near-surface, three-dimensional (3-D) electrical inhomogeneity. The effects of this local galvanic distortion should be separated and removed from the regional response to improve the accuracy and reliability of the data interpretation. In this paper, it is attempted to introduce an effective form of tensor analysis to facilitate the process of GB (Groom-Bailey) tensor decomposition on MT data. This approach was used to recover the regional response of conductivity structures beneath 12 MT sounding sites of a sedimentary basin in South Australia. The results of this study clearly indicate that the regional structures beneath these sites are two-dimensional (2-D) and their strike are mainly in NS ($\pm 10^0$) direction which are geologically supported. The obtained results also show that the distortion parameters of the surficial bodies are fairly constant for the whole frequency band or its two or, at most, three subsets. In addition, the low misfit values between the measured impedances and those produced by a hypothetical 3D/2D model confirm that the regional structures beneath all these 12 MT sites are 2-D and some local surficial 3-D features are superimposed on them.

Keywords: impedance tensor, near-surface inhomogeneity, regional structure, tensor analysis, tensor decomposition, galvanic distortion

1 Introduction

Magnetotelluric is a natural source electromagnetic method that involves measuring fluctuations in the natural electric (E) and magnetic (H) fields in orthogonal directions at the earth's surface. The main aim of the MT exploration is to determine the conductivity structure of the earth at depths ranging from a few tens of meters to several tens of kilometers. The

*Corresponding author: a_moradzadeh@ut.ac.ir

relationship between the orthogonal components of the horizontal electric and the magnetic field vectors at a single MT site in the frequency domain is normally represented by,

$$\mathbf{E} = \mathbf{ZH}. \quad (1)$$

In Cartesian coordinates (x,y,z), this can be written out as follows:

$$\begin{pmatrix} E_X \\ E_Y \end{pmatrix} = \begin{pmatrix} Z_{XX} & Z_{XY} \\ Z_{YX} & Z_{YY} \end{pmatrix} \begin{pmatrix} H_X \\ H_Y \end{pmatrix} \quad (2)$$

where $\mathbf{Z}(\omega)=\begin{pmatrix} Z_{XX} & Z_{XY} \\ Z_{YX} & Z_{YY} \end{pmatrix}$ is a complex MT impedance tensor or transfer function and is defined for each frequency (f). In the one-dimensional (1-D) or horizontal-layered earth structures, Zxx=Zyy= 0, and Zxy = –Zyx, i.e.

$$Z_{1-D} = \begin{pmatrix} 0 & Z_1 \\ -Z_1 & 0 \end{pmatrix} \quad (3)$$

In the presence of 2-D structures in the subsurface, if one of the measurement axes (x,y) is along the strike, then the diagonal elements of Z(ω) get a zero value while Zxy ≠ Zyx, i.e.

$$Z_{2-D} = \begin{pmatrix} 0 & Z_{xy} \\ Z_{yx} & 0 \end{pmatrix} \quad (4)$$

otherwise, or when the subsurface structures are 3-D, none of the impedance elements is zero.

Since the strike direction of an anomaly is seldom known at the time of a field survey, the field sensors are oriented along arbitrary axes (x,y). To determine the strike of the conductivity structure, an attempt is then made to eliminate diagonal elements of the impedance tensor. However, if the conductivity tensor is not symmetric or some noise is present, these elements do not vanish. In such cases, an attempt is made to minimise the diagonal elements. To achieve this, the measured impedance tensor is rotated (Swift, 1967; Vozoff, 1991) through a positive angle θ as follows:

$$\mathbf{Z}'(\theta) = \mathbf{R}\,\mathbf{Z}\,\mathbf{R}^{T} \quad (5)$$

where $\mathbf{R} = \begin{pmatrix} \cos\theta & \sin\theta \\ -\sin\theta & \cos\theta \end{pmatrix}$ is the rotation matrix, $\mathbf{R}^T$ is its transpose, and θ is the rotation angle in the clockwise direction. The rotation angle (θ) is chosen such that Z′(θ) takes an approximately zero-diagonal form, i.e.

$$\mathbf{Z}'(\theta_0) = \begin{pmatrix} 0 & Z'_{XY} \\ Z'_{YX} & 0 \end{pmatrix} \quad (6)$$

The off-diagonal elements of $\mathbf{Z}'(\theta_0)$ are known as the principal components of the impedance tensor. The directional apparent resistivity (ρ'_{xy}, ρ'_{yx}) and rge phase (φ'_{xy}, φ'_{yx}) values of each period (T) are given by the real and imaginary components of the rotated impedance tensor ($\mathbf{Z}'(\theta_0)$) in the following forms (Moradzadeh, 1998):

$$\rho'_{xy} = 0.2\,T\,|\,Z'_{xy}|^{2}\ ,$$
$$\varphi'_{xy} = \tan^{-1}(\mathrm{Im}\,Z'_{xy} / \mathrm{Re}\,Z'_{xy})$$
$$\rho'_{yx} = 0.2\,T\,|\,Z'_{yx}|^{2}\ ,$$
$$\varphi'_{yx} = \tan^{-1}(\mathrm{Im}\,Z'_{yx} / \mathrm{Re}\,Z'_{yx}) \quad (7)$$

where the phase of impedance (φ) varies from 0 to 90 degrees.

One of the major problems in the interpretation of the magnetotelluric data is the effects caused by topographical features or near-surface 3-D inhomogeneities. Such small local features create a charge on the conductivity boundaries and thus cause galvanic distortion of the measured electric and magnetic fields (Larsen, 1977; Berdichevsky and Dmitriev, 1976; Zhang et al., 1987; Bahr, 1988; Groom and Bailey,1989; Lilley and Weaver, 2010). This galvanic response (due to boundary charges) that is essentially independent of frequency within the range of an MT sounding (Berdichevsky and Dmitriev, 1976) causes the measured electric fields to be perturbed from their regional values and a shift of the apparent resistivity curves take place vertically in a log-log scale of apparent resistivity sounding curves. The impedance phase, however, is unaffected. This is called the MT static shift and it needs to be minimised somehow to allow an accurate interpretation of data. Therefore, galvanic distortion can be regarded as the superposition of the signatures of such localized, near-surface 3-D heterogeneities on the signature of the larger-scale regional structure. Such distortion can mask the properties of the larger-scale structure that is the usual target of the MT surveys (Bibby et al., 2005; Kannaujiya and Israil, 2012). It is shown that the distortion effects on the electric field are more severe than that of the magnetic field.

The local distortion of the electric field and its effects on the regional MT impedance tensors can be corrected by different tensor decomposition methods (e.g. Larsen,1977; Eggers,1982; LaTorraca et al.,1986; Zhang et al., 1987; Yee and Paulson, 1987; Chauteau and Bouchard, 1988; Jiracek et al., 1989; Bahr, 1988, 1991; Groom and Bailey, 1989, 1991; Chakridi et al., 1992; Chave and Smith, 1994; Lilley, 1995, 1998, 2012, Li et al., 2010). In all these methods, it is assumed that the regional structure is 1-D or 2-D and a surficial small 3-D anomalous body which is smaller than the skin depth of the EM waves overlay them. In addition to these methods, the MT phase tensor analysis has been used by many researchers to cure this problem (e.g., Caldwell et al., 2004; Bibby et al., 2005; Booker, 2014). Some of these methods like Bahr (1988) decomposition approach and phase tensor methods are very sensitive to the noise in data and give unstable solutions. It is also difficult to realize an optimised decomposition of phase tensors for a multi-frequency equation. Whereas the Groom and Bailey (1989, 1991) tensor decomposition, hereafter referred to as GB, uses an efficient optimisation technique to simultaneously determine the regional impedance elements and distortion factors for multi-frequency data. Although, this method is very complicated to be used in practical MT studies, it has a better stability with respect to the Bahr decomposition and phase tensor method. A comparison of the efficiency of some of the above methods was given by Groom and Bailey (1991) and Cai et al., (2010) for both synthetic and real MT data.

Considering the aforementioned material and importance of the problem, the objective of this study was to remove the influences of the near-surface 3-D heterogeneities from the measured MT

impedance tensor and hence determine the impedance tensor that only represents the effects of the regional structure. This is done by introducing a simple form of tensor analysis to simplify the complicated decomposition of MT impedance tensor. However, the physical reasons for this phenomenon are described first, then the measured MT impedance tensors are analysed using a hypothetical 3D/2D (small 3-D body over a 2-D regional structure) physical model.

2 Physics of distortions

Before using some techniques to reduce the distorting effects of the near-surface inhomogeneities on the present data set, a brief physical description of the phenomena is presented. Distorting effects on MT fields can be classified as galvanic and inductive (Berdichevsky and Dmitriev, 1976; Zhdanov, 1987; Kuafman, 1988; Smith, 1995). Here distribution of EM fields in layered earth is termed primary, and any distortion of these fields is called secondary (anomalous) fields. Consequently, the total fields at any point on the surface of the earth can be represented as:

$$\mathbf{E} = \mathbf{E}_P + \mathbf{E}_S \qquad \mathbf{H} = \mathbf{H}_P + \mathbf{H}_S \qquad (8)$$

where $\mathbf{E}_P$ and $\mathbf{H}_p$ are electric and magnetic primary fields in a horizontally layered earth, while $\mathbf{E}_s$ and $\mathbf{H}_s$ are secondary fields due to inhomogeneity. These secondary fields can, in turn, contain both galvanic and inductive components. However, later it will be shown that the inductive effect of such small near-surface bodies is negligible for low frequencies and can safely be neglected. The physical explanation of galvanic and inductive phenomena is given in the following section.

If one component of the electric field is in the direction of the conductivity gradient, some charges are built up on the boundaries of the inhomogeneities. According to Ohm's law ($\mathbf{J}=\sigma\mathbf{E}$) and the current continuity equation, the volume charge density ρ_v in a conductive medium can be given (Pellerin, 1988) as:

$$\rho_v = \varepsilon_0 /(\sigma + i\omega\varepsilon_0)\ \mathbf{E}.\nabla\sigma \qquad (9)$$

which by applying the quasi-static approximation ($\sigma >> \omega\varepsilon_0$) becomes

$$\rho_v = \varepsilon_0 /\sigma\ \mathbf{E}.\nabla\sigma \qquad (10)$$

where ω is the angular frequency, σ is the conductivity of earth material, and ε_0 is the dielectric permittivity of free space.

From Eq. (10) it can clearly be seen that the charge density is independent of the frequency. For areas with sharp conductivity contrast, ρ_v reduces to the surface charge density ρ_s (Jiracek, 1990). The secondary electric field due to these charges can be calculated (LeMouel and Menvielle, 1982) using the following expression.

$$\mathbf{E}_s = -\partial\mathbf{A}_s/\partial t - \nabla\varphi \qquad (11)$$

where $\mathbf{A}_s$ is the secondary magnetic vector potential of boundary charges and φ is the electrostatic scalar potential. By taking the time dependence of $e^{i\omega t}$, the secondary (scattered) electric field can be defined as the integral of the scattering currents within the anomalous zone weighted by background Green's function (Hohmann, 1975; Groom and Bahr, 1992).

$$\mathbf{E}_s(\mathbf{r}) = i\omega\mu_0 \int_v g(\mathbf{r}, \mathbf{r}_s)\, \delta\sigma\, \mathbf{E}(\mathbf{r}_s)\, dv + 1/\sigma_0\, \nabla\nabla . \int_v g(\mathbf{r}, \mathbf{r}_s)\, \delta\sigma\, \mathbf{E}(\mathbf{r}_s)\, dv \quad (12)$$

where g is scalar Green's function for the background and $\delta\sigma = (\sigma_a - \sigma_0)$ is the conductivity difference between the anomalous zone (σ_a) and the background (σ_0). The volume of inhomogeneity is represented by v, and **r** is an arbitrary measurement point while $\mathbf{r}_s$ is a source point in the anomalous body.

For small inhomogeneities at the low-frequency limit, the first part of the above equation can be ignored and in an area with sharp conductivity contrast, the secondary electric field is given by Coulomb's law,

$$\mathbf{E}_s = -\frac{1}{4\pi\varepsilon_0} \int_s \frac{\rho_s}{|r|^2} r_0 ds. \quad (13)$$

Here **r** is a vector between the measurement point and the element of *ds*, and $\mathbf{r}_0$ is a unit vector of **r**.

At low frequencies in which the penetration depth of EM field is much greater than the size of near-surface bodies, the galvanic distortion of the magnetic field can be neglected (Wannamaker et al., 1984). Therefore, due to galvanic distortion by the electric field, the MT apparent resistivity curve in a log-log plot of the apparent resistivity versus frequency is shifted upward or downward (depending on the type of inhomogeneity) by a frequency independent scale factor. This effect is called static shift or S-effect in the MT survey. When the background electric field is distorted by a small near-surface body, an anomalous (secondary) current is created which in turn creates an anomalous magnetic field. This magnetic field of the galvanic scattering is given (Groom and Bahr, 1992) by

$$\mathbf{H}_s = \nabla \times \int_v g(\mathbf{r}, \mathbf{r}_s)\, \delta\sigma\, \mathbf{E}(\mathbf{r}_s)\, dv. \quad (14)$$

Although the magnetic field due to galvanic scattering is not significant for small bodies at the low-frequency limit, its effects could be significant for large galvanic distortion or when the frequency is sufficiently high. As the secondary galvanic electric field is in-phase with the uniform primary charging field and for low frequencies the secondary magnetic field is insignificant, the impedance phase data are not distorted (Moradzadeh, 1998).

The inductive effect follows Faraday's law, where the time-varying magnetic field induces a vortex of excess electrical currents and these eddy currents, in turn, produce the secondary magnetic field $\mathbf{H}_s$. These secondary fields distort the primary magnetic field. To understand the inductive distortion effect, the induction number (a dimensionless quantity defined in free space) is utilised. By a quasi-static approximation, this quantity for a sphere with radius R is given (Ward, 1967) by:

$$K = (\omega\mu_0\sigma)^{1/2} R \quad (15)$$

where ω is the angular frequency, μ_0 is the free space magnetic permeability, and σ is the conductivity of the body. Through this equation, it can be seen that the inductive response of a body is a function of frequency, its electrical properties and geometry. In contrast to the galvanic effect, the secondary and primary magnetic fields are not in-phase. The phase shift changes from 0 (for the highest K) to $\pi/2$ (for the

lowest K). Equation (15) also shows that in the range of low frequencies, the inductive effect of a small near-surface body is not as important as the galvanic effect in MT exploration. However, when a 2-D surface body is embedded in a layered earth, its transverse electric (TE) polarisation mode response is highly distorted and can cause a false conductive layer on the TE apparent resistivity curve (Berdichevsky and Dmitriev, 1976; Berdichevsky and Zhdanov, 1984). As a conclusion, the effects of any small-scale shallow inhomogeneity structure on the MT data may include: producing a static shift on resistivity curves, distortion of the regional impedances and may change the phase of the regional impedance tensors due to an anomalous magnetic field at sufficiently high frequencies.

3 Analysis and decomposition of the impedance tensor

A comprehensive study on a MT data set (including 38 MT sites of two profiles) within South Australia (Moradzadeh, 1998; Moradzadeh and White, 2005) indicates that the regional structures of the area are 2-D, and the regional strike direction for most of the MT sites is in the NS ($\pm 5^0$) direction which agrees well with the general geological trend in this area (Figure 1). However, the dimensionality and strike of a few (12) sites are different, i.e. NS ($\pm 30^0$) and also not in agreement with the general geological trend of the area. This may be due to the effects of near-surface 3-D bodies. Therefore, in these sites, the calculated strike angles probably reflect the local azimuth of these near-surface 3-D features instead of the regional strike direction. This idea is also supported by the results of the second profile which show that the regional strike direction is NS ($\pm 10^0$) under all its MT sites (except MOU). The effects of these local 3-D near-surface inhomogeneities need to be minimised to recover the correct regional impedance tensor for the further analysis of the data. These 12 MT sites include YAD, OAK, DAW, ODD, MAN, PIT, MAF, MUL, LWD, SWD, MAD, and MOU that are located within a complex sedimentary basin, wherein the near surface conductivity inhomogeneity is a common phenomenon in the sedimentary environment. Consequently, it is assumed that the regional structure is 2-D and it is superimposed by small-scale 3-D surfacial bodies, i.e. the 3-D local/2-D regional composite model is assumed. Hence, the GB method is applied to test this hypothesis and to extract the correct regional geoelectrical strike and impedance elements from the galvanically distorted measured impedance. However, prior to using such a complicated analysis and to facilitate the process and also to test whether any distortion is present in the data, a simple tensor analysis was carried out on the data.

It was shown that the measured impedance tensor ($\mathbf{Z}_m$) can be related to the regional tensor ($\mathbf{Z}_r$) through a 2×2 real electric distortion matrix $\mathbf{C}$, e.g. $\mathbf{Z}_m = \mathbf{C}\,\mathbf{Z}_r$. If $\mathbf{Z}_r$ is 2-D and the measurements are along the principal axes, then $\mathbf{Z}_m$ is given as (Bahr, 1988):

$$Z_m = \begin{pmatrix} c_{xx} & c_{xy} \\ c_{yx} & c_{yy} \end{pmatrix} \begin{pmatrix} 0 & Z_{xy} \\ Z_{yx} & 0 \end{pmatrix} = \begin{pmatrix} c_{xy} Z_{yx} & c_{xx} Z_{xy} \\ c_{yy} Z_{yx} & c_{yx} Z_{xy} \end{pmatrix} \tag{16}$$

In such cases, the elements of each column of $\mathbf{Z}_m$ have identical phase, but their magnitudes differ by a real factor. If Z_r is 2-D and measurements are in arbitrary coordinates, $\mathbf{Z}_m$ can be given as:

$$\mathbf{Z}_m = \mathbf{R}\,\mathbf{C}\,\mathbf{Z}_{2D}\,\mathbf{R}^T \qquad (17)$$

where $\mathbf{R}$ is a rotation matrix, $\mathbf{R}^T$ is its transpose, and $\mathbf{Z}_{2D}$ is the regional 2-D impedance tensor in the principal direction. In this case, each element of $\mathbf{Z}_m$ has its own phase and magnitude.

To determine the regional strike direction, $\mathbf{Z}_m$ is rotated stepwise until the phases coincide column by column (Moradzadeh, 1998). Such analyses were carried out on data of 12 sites, and the regional strike was found to be in the NS ($\pm 10^0$) direction. Figure 2 illustrates the results for one of these sites as a representative example of such analyses. The high resistivity values corresponding to the xx and yy elements of the impedance tensor clearly confirm the presence of a 3-D galvanic distortion.

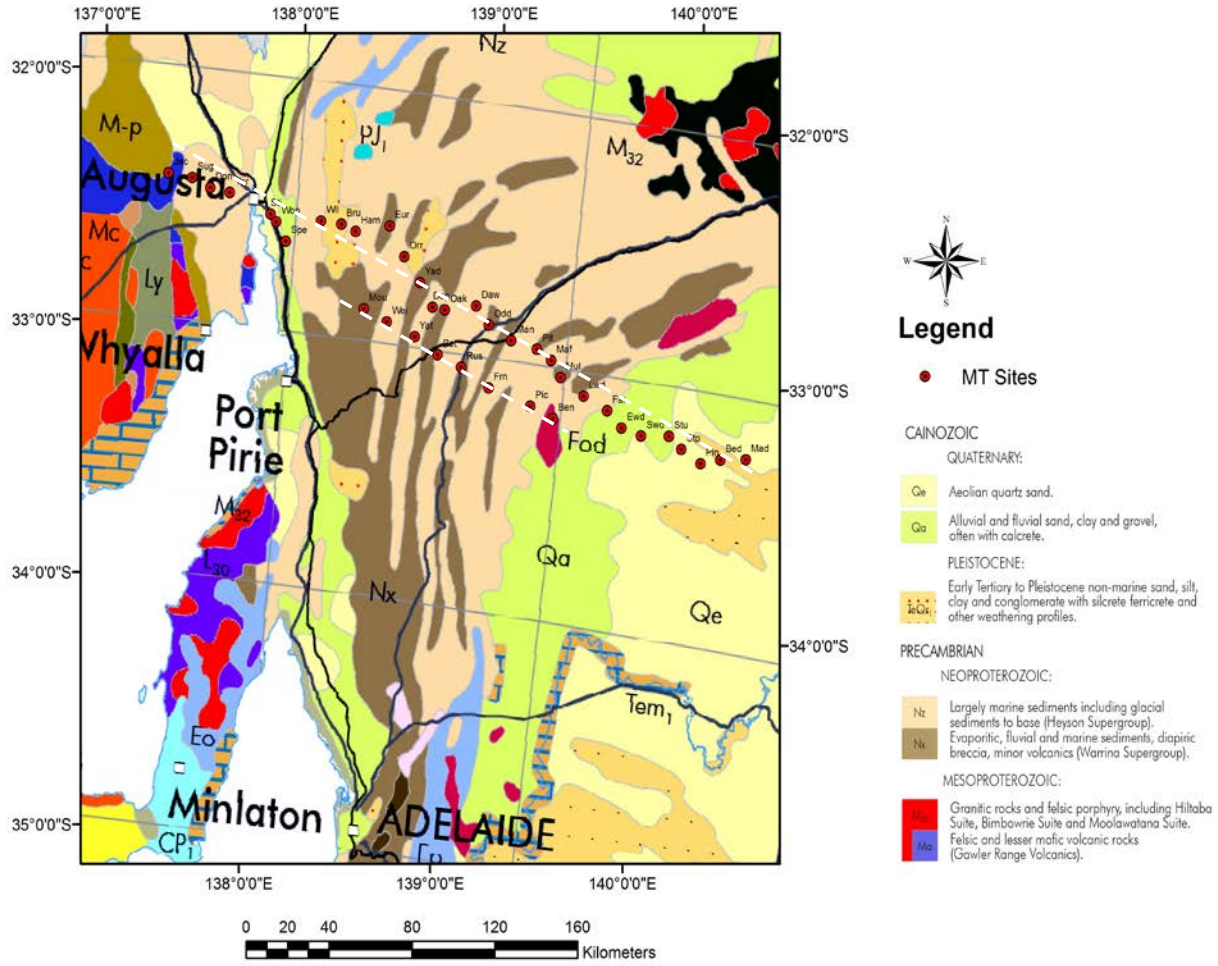

Figure 1. The general geological map of the area including MT sites (red circles) along two parallel profiles which have been shown as white dashed lines (after Cowley, 2010).

The same phases for xx and yx and also the same phases for xy and yy elements indicate that the measurement axes (NS) happen to coincide with the regional 2-D principal directions.

To confirm the results of our tensors analysis and to reduce 3-D distortion effects on data, the GB decomposition method was then applied to the data of aforementioned sites. In this method, the distortion matrix **C** is factorised into three tensors: anisotropy (**A**), shear (**S**), and twist (**T**) which are multiplied by a real factor g (site gain), viz.

$$C = g\mathbf{T}\,\mathbf{S}\,\mathbf{A} = g\begin{pmatrix}1 & -t\\ t & 1\end{pmatrix}\begin{pmatrix}1 & e\\ e & 1\end{pmatrix}\begin{pmatrix}1+s & 0\\ 0 & 1-s\end{pmatrix} \quad (18)$$

where *s* is the anisotropy factor, *t* and *e* are tangents of the electric field twist and shear angles, respectively.

Thus, the measured impedance tensor is given as:

$$\mathbf{Z}_m = \mathbf{R}\,\mathbf{T}\,\mathbf{S}\,[\,g\mathbf{A}\,\mathbf{Z}_{2D}\,]\,\mathbf{R}^T \quad (19)$$

This equation provides eight non-linear real equations with seven real unknown parameters (twist and shear as two distortion parameters, regional strike angle, and the remaining four are two complex 2-D regional impedances scaled by real the factor gA). Among these, the site gain (g) cannot be determined based on only MT data and its correction was addressed to Moradzadeh (2003); however, in this study, s (local anisotropy) is evaluated by requiring high frequency asymptotes of both modes of apparent resistivity to be equal (Jones and Dumas, 1993; Groom et al., 1993). This is because the phase values of both polarisation modes are the same for high frequencies (i.e. f > 1Hz) which indicates the shallow structure is almost 1-D beneath most of the sites.

It should be noted that making use of the GB decomposition technique on the data of a single-site single-frequency impedance tensor, we are only able to uniquely recover the regional strike θ_{reg2D}, the directional distortions twist *t*, the shear *e*, and the scaled regional impedances, $Z_{xy}^{scaled}, Z_{yx}^{scaled}$.

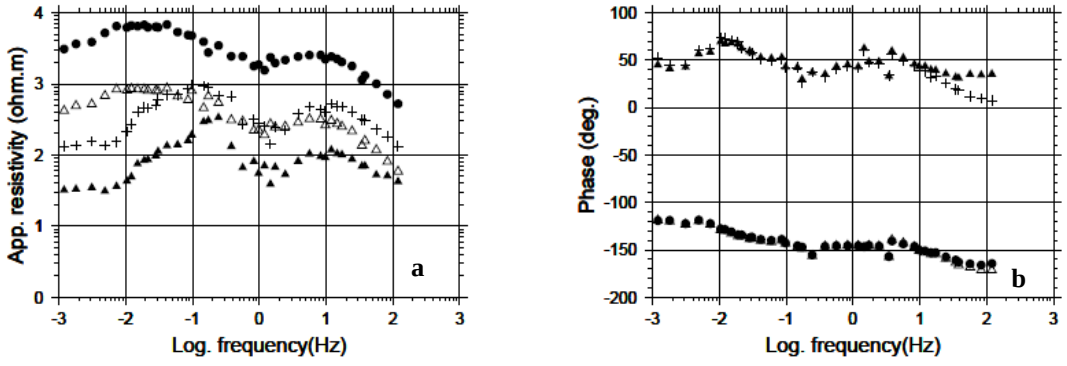

Figure 2. (a) Logarithm of apparent resistivity and (b) phase data for MAN in the NS direction. All apparent resistivity and phase values corresponding to xx (blank triangles), yx (solid circles), xy (solid triangles), and yy (crosses) elements of the impedance tensor have been shown in the figure.

This method of decomposition leads to the solution of a system of eight real, non-linear algebraic equations that result from the conditions of fitting the experimental impedances to those produced by the composite model (Cerv et al., 2010),

$$Z_m^{model} = R(\theta_m - \theta_{reg\,2D}) \begin{pmatrix} 1-te & e-t \\ e+t & 1+te \end{pmatrix} \begin{pmatrix} 0 & Z_{xy}^{scaled} \\ Z_{yx}^{scaled} & 0 \end{pmatrix} R(\theta_{reg\,2D} - \theta_m), \quad (20)$$

where R(θ) is a 2-D rotation matrix through θ.

Practically, the above mentioned seven unknown parameters are determined statistically by requiring that the misfit between the model and data is minimised. To assess the goodness of the fit, a number of tests such as the chi-squared (χ^2) -like normalised residual misfit (Groom et al., 1993) and the standard χ^2 (Chave and Jones, 1997) can be used. However, the latter one (with the assumption of normally distributed errors in the tensor elements) was used in this study. As a criteria to test the appropriateness of the proposed 3D/2D model, the χ^2 misfit is required to be less than 4 (if none of the parameters is constrained). In addition, the distortion parameters (twist and shear) must be independent of the frequency for the whole frequency band or at least for some of its subsets. In the GB-method estimates of the regional parameters, and especially those of the regional strike θ_{reg2D} are often unstable and largely scattered if they are evaluated separately for individual frequencies within some frequency range. This problem is resolved by the proposed method of a tensor analysis prior to the GB decomposition. In a procedure by McNeice and Jones (2001), the observed impedance data are fitted by a composite model for a whole range of periods and for multiple sites, simultaneously.

4 Results and discussion

This section describes how the proposed tensor analysis and decomposition of the impedance tensor are successful in reducing the effects of the surficial small-scale inhomogeneities on the data. As noted previously, the galvanic distortion of the electric field requires the seven parameters (two regional complex response functions, twist, shear, and regional strike) to be fitted to eight data points at each frequency in the least squares sense. Thus, the χ^2 test has only one degree of freedom, so that the χ^2 expected value is 1, while its value is 3.84 for a 95% confidence limit. If one of these seven parameters is constrained to be constant for all frequencies, then six parameters are fitted at each frequency plus one parameter is fitted simultaneously for all frequencies; therefore, the degree of freedom is slightly less than 2 and the χ^2 value for a 95% limit is 5.991 (≈6.0). In addition, if the strike and both of the distortion parameters are constrained to be constant for the entire range of frequency, then there are only four parameters at each frequency plus three parameters which must be fitted simultaneously for all frequencies to eight data points; hence, the degree of freedom will be slightly fewer than 4 and the corresponding 95% value for the χ^2 test will be 9.49.

During the decomposition, it is usual that one, two or even three parameters are constrained so that one gets a smoother model; however, this procedure may increase the misfit. Therefore, any increase in the misfit associated with any smoothing must be evaluated to assess whether the constrained model is supported by the data. It is concluded that a compromise must be made between minimising the misfit and maximising smoothness (Groom et al., 1993). The GB decomposition for the galvanic distortion of the electric field has been performed using the program provided by Chave and Smith (1994).
The preliminarily tensor analysis indicates that the strike direction of the regional structures beneath these twelve distorted sites are as in Table 1.

Sites code	MAN	YAD	OAK	DAW	ODD	PIT	MAF	MUL	LWD	SWD	MAD	MOU
Strike (deg)	0	-10	0	0	0	5	-15	5	-10	5	-10	10

Table 1. Strike direction based on the proposed tensor analysis.

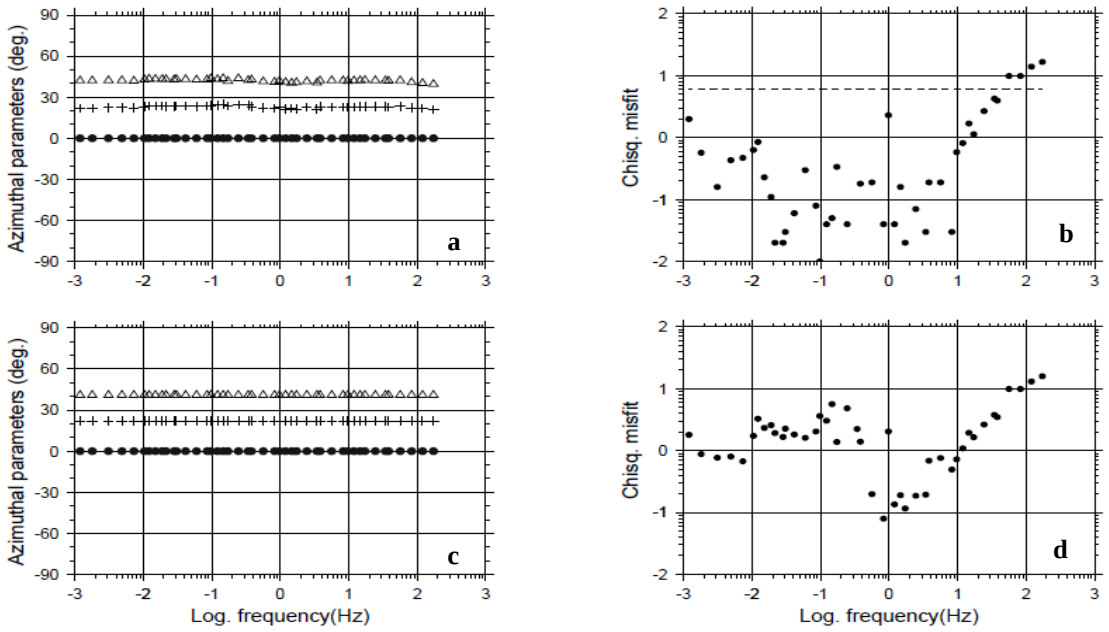

Figure 3. The results of the GB decomposition for the MAN data. GB parameterisation with strike (solid circle) constrained to 0^o (a and b). The results of the full constrained GB parameterisation of this site with the twist (crosses) $=22^0$ and shear (triangles) $= 41^0$ are given in (c) and (d).The logarithm of χ^2 misfit is given in figures 3b and 3d.

Then as a starting point for the GB decomposition, the regional strike was constrained according to the values in the above table. Figures 3a and 3b show the results of the GB decomposition for the site MAN when the strike is constrained to 0°. From the figure, it is quite evident that both twist (crosses) and shear (triangles) are relatively constant over the whole frequency range and also the χ^2 misfit is less than 6 for frequencies less than 60 Hz. In the next stage of the decomposition, in addition to the strike, both twist and shear were constrained to 22° and 41°, respectively (Figure 3c). The value of misfit is also less than 9.49 (Figure 3d) for all frequencies except for a few points at very high frequencies. Therefore, the proposed local 3-D over a regional 2-D (3D/2D) model is supported for this site. The GB decomposition was applied to the data of the remaining 11 sites. The results for some of them are shown in Figures 3 through 7.

The appropriateness of 3D/2D model can also be judged using the comparison of the plots of the observed data and the model response. Figure 8 illustrates such a plot for the site MAD as an example. From this figure, it can be seen how the observed real and imaginary elements of the impedance tensor are fitted to their corresponding values of the model response. The results of this study (e.g. Figures 3 to 8) clearly indicated that the distortion parameters are fairly constant for the whole frequency band or its two or, at most, three subsets. In addition, the low misfit values confirmed that the regional structure beneath all these 12 MT sites was two-dimensional and some local near surface 3-D features were superimposed on them.

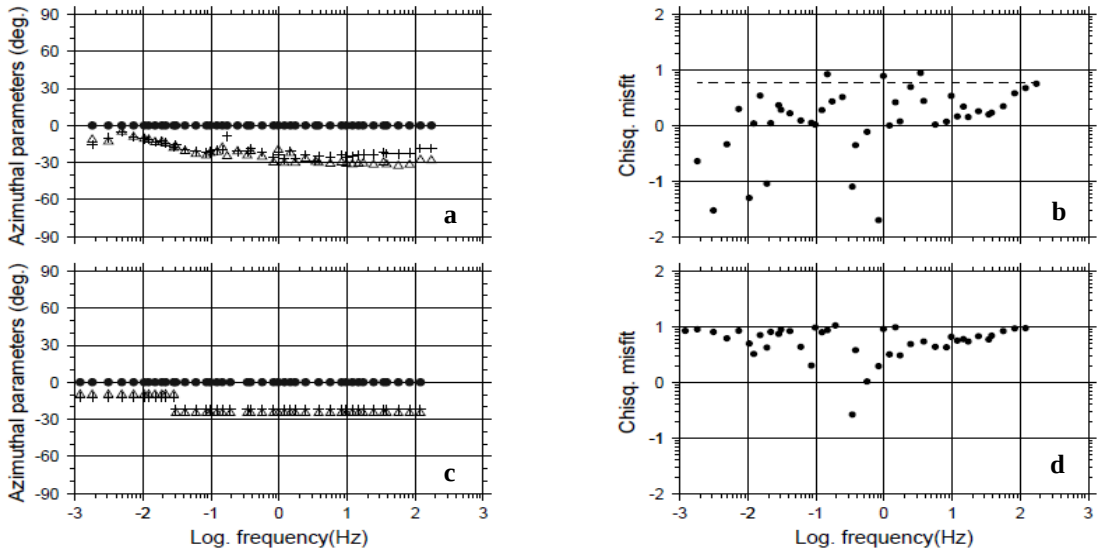

Figure 4. The results of the GB decomposition for the DAW data with the strike (solid circles) constrained to 0^o (a and b). The results of the full constrained GB parameterisation of this site with twist (crosses) = -12°, and -22° and shear (triangles) = -10°, and -25° (from low to high frequency bands, respectively) are given in (c) and (d). The logarithm of χ^2 misfit is given in figures 4b and 4d.

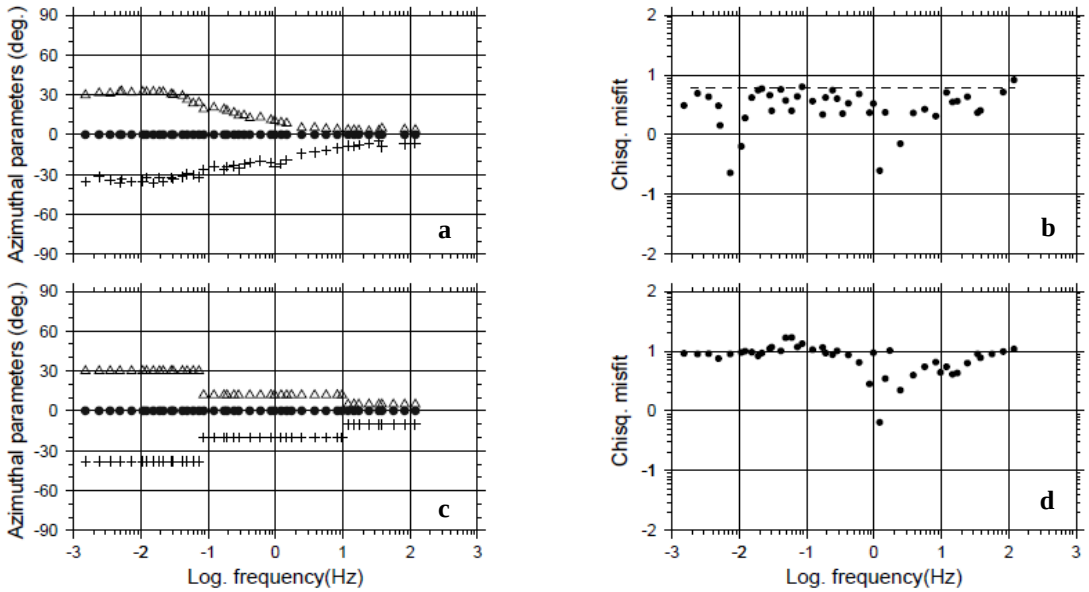

Figure 5. The results of the GB decomposition for the ODD data. GB parameterisation with the strike (solid circle) constrained to 0^o (a and b). The results of the full constrained GB parameterisation of this site with twist (crosses) = -38°, -20°, and -10° and shear (triangles) = 30°, 12°, and 5° (from low to high frequency bands respectively) are given in (c) and (d). The logarithm of χ^2 misfit is given in figures 5b and 5d.

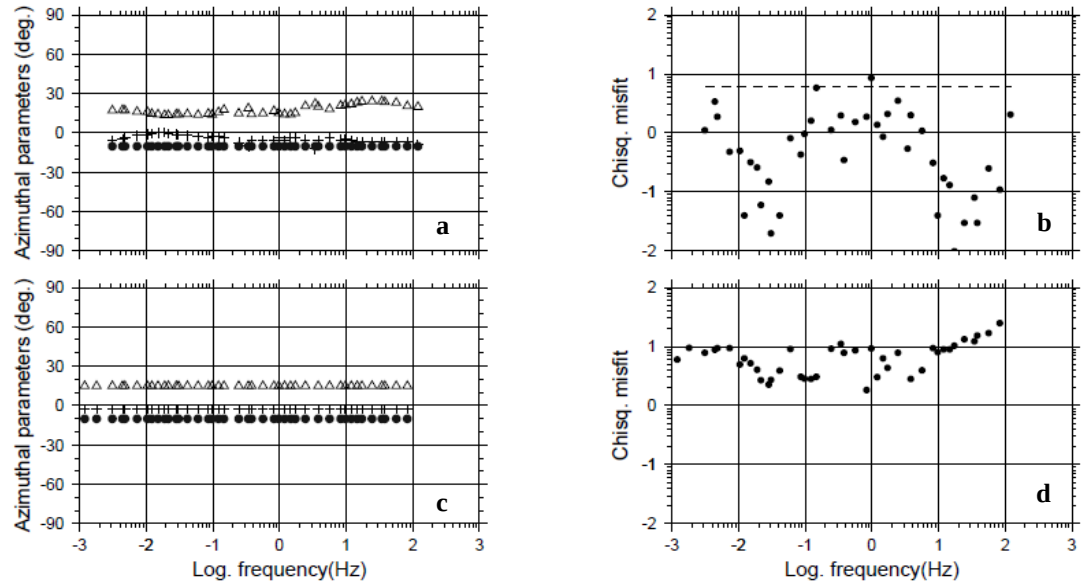

Figure 6. The results of the GB decomposition for LWD data. GB parameterisation with the strike (solid circles) constrained to -10^o (a and b). The results of the full constrained GB parameterisation of this site with twist (crosses) = -2.5°, and shear (triangles) = 15° are given in (c) and (d). The logarithm of χ^2 misfit is given in figures 6b and 6d.

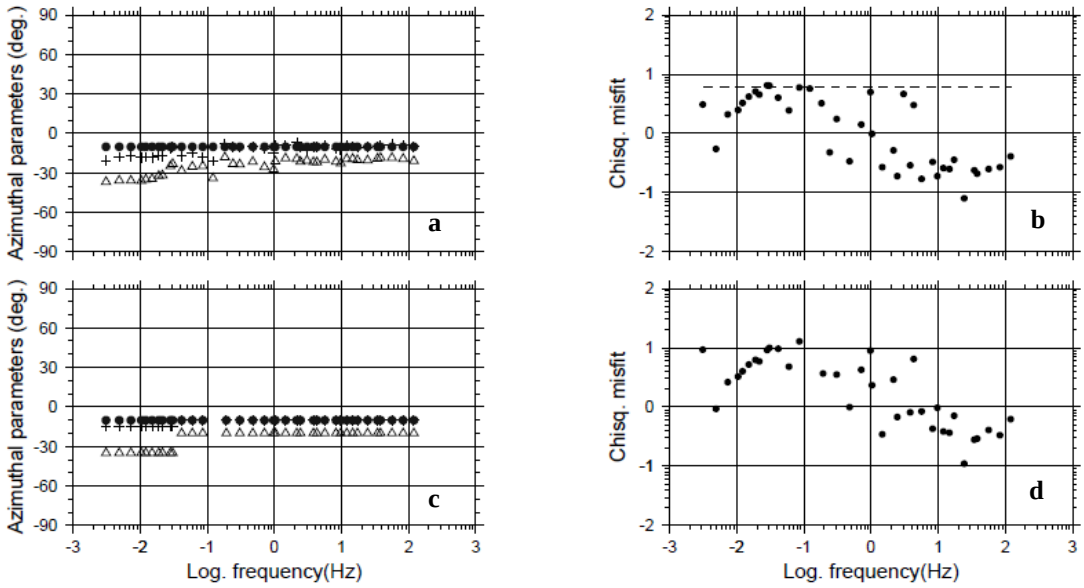

Figure 7. The results of the GB decomposition for MAD data with the strike (solid circle) constrained to -10° (a and b). The results of the full constrained GB parameterisation of this site with twist (cross) = -15°, and -10° and shear (triangles) = -35°, and -20° (from low to high frequency bands respectively) are given in (c) and (d). The logarithm of χ^2 misfit is given in figures 7b and 7d.

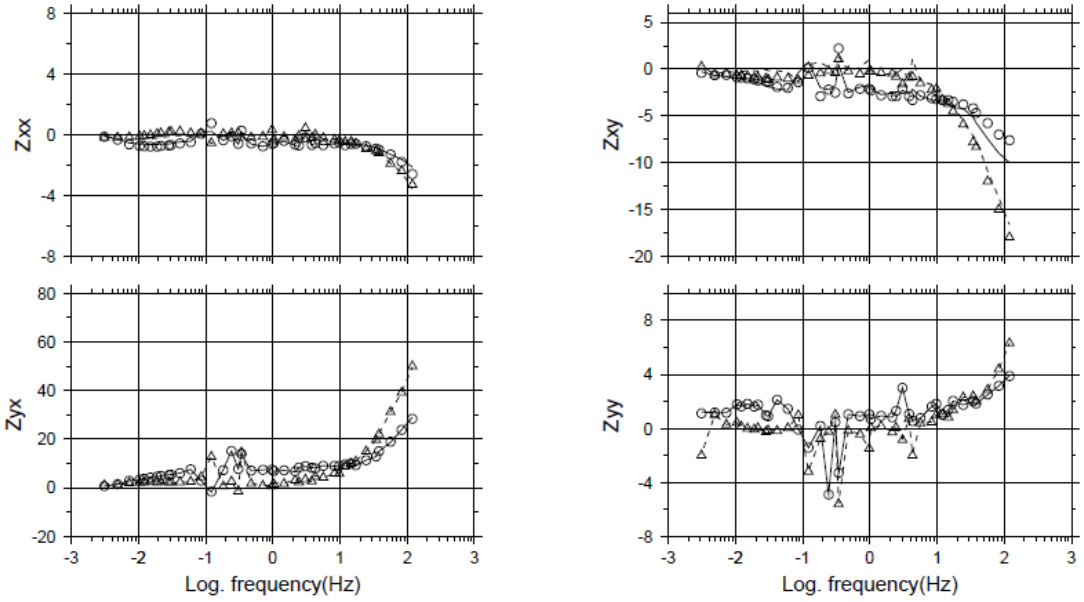

Figure 8. The GB parameterisation fit to the data of the MAD. Solid and dashed lines stand for real and imaginary response of the GB model. Circles and triangles denote real and imaginary parts of observed data (e.g. impedance tensor), respectively.

5. Conclusions

Various forms of analyses on the estimated impedance tensors of the 38 MT data sets of a sedimentary basin within the South Australia indicated that the regional structures were two-dimensional with a NS ($\pm 5^0$) strike direction for most sites. However, the dimensionality and strike of 12 MT sites were different. In this study, a simple form of the tensor analysis showed that the differences were due to distortion from local 3-D near surface inhomogeneities. Thus, when the regional strike of the subsurface structure of these 12 MT sites was determined by the introduced tensor analysis, the MT impedance tensors of these distorted sites were decomposed using the GB method to extract the correct regional impedance elements of subsurface structures. The obtained results of the tensor analysis and the GB decomposition indicated that the strike of the regional 2-D structure beneath 11 sites were in the NS ($\pm 10^0$) direction while it was -15^0 below MAF. The resultant regional strike direction under these MT sites was consistent with the results given at the other sites. It was also supported geologically. Considering the results, it could be concluded that a combination of the proposed simple tensor analysis and the GB tensor decomposition was properly able to recover the strike of a 2-D regional structure and its correct values of impedance tensor which could be used for further interpretations.

Acknowledgments

The programs related to the dimensionality and tensor analysis of the impedance tensor have been written by the author, but for computer codes regarding the GB decomposition, I would like to thank Drs Chave and Smith (1994) who kindly provided the required computer codes.

References

Bahr, K., 1988, Interpretation of the magnetotelluric impedance tensor; regional induction and local telluric distortion: J. Geophys., **62,** 119-127.

Bahr, K., 1991, Geological noise in magnetotelluric data; a classification of distortion types: Phys. Earth Planet. Inter., **66,** 24-38.

Berdichevsky, M. N. and Dmitriev, V. I., 1976, Basic principles of interpretation magnetotelluric sounding curves: Geoelectric and Geothermal Studies, 165-221. Budapest.

Berdichevsky, M. N. and Zhdanov, M. S., 1984, Advanced theory of Deep Geomagnetic Sounding: Elsevier, 408.

Bibby, H. M. Caldwell, T. G. and Brown, C., 2005, Determinable and non-determinable parameters of galvanic distortion in magnetotellurics: Geophys. J. Int., **163,** 915–930.

Booker, J. R., 2014, The magnetotelluric phase tensor: A Critical Review: Survey in Geophysics, **35,** 7–40.

Cai, J. T., Chen, X. B. and Zhao, G. Z., 2010, Refined techniques for data processing and two-dimensional inversion in magnetotelluric I; Tensor decomposition and dimensionality analysis: Chinese J. Geophys., **53 (6),** 1060-1071.

Caldwell, T. G., Bibby, H. M. and Caldwell, C., 2004, The magnetotelluric phase tensor: Geophys. J. Int.,**158**, 457–469.

Cerv, V., Pek, G. and Menvielle, M., 2010, Bayesian approach to magnetotelluric

tensor decomposition: Annals of Geophysics, **53 (2),** 21-32.

Chakridi, R., Chouteau, M. and Mareschal, M., 1992, A simple technique for analysing and partly removing galvanic distortion from the magnetotelluric impedance tensor; application to Abitibi and Kapuskasing data (Canada): Geophys. J. Int., **108,** 917-929.

Chave, A. D. and Smith, J. T., 1994, On electric and magnetic galvanic distortion tensor decompositions: J. Geophys. Res., **99,** 4669-4682.

Chave, A. D. and Jones, A. G., 1997, Electrical and magnetic field galvanic distortion decomposition of BC87 data: J. Geomag. Geoelectr., **49,** 767-789.

Chouteau, M. and Bouchard, K., 1988, Two-dimensional terrain correction in magnetotelluric surveys: Geophysics, **53,** 854-862.

Cowley, W., 2010. Summary geology of South Australia, Government of South Australia, Department of State Development, South Australia Earth Resources information sheet, M51, 1-11.

Eggers, D. E., 1982, An eigenstate formulation of the magnetotelluric impedance tensor: Geophysics, **47,** 1204 - 1214.

Groom, R. W. and Bailey, R. C., 1989, Decomposition of magnetotelluric impedance tensors in the presence of local three-dimensional galvanic distortion: J. Geophys. Res., **94,** 1913-1925.

Groom, R. W. and Bailey, R. C., 1991, Analytic investigations of the effects of near-surface three-dimensional Galvanic scatterers on MT tensor decompositions: Geophysics, **56,** 496-518.

Groom, R. W. and Bahr, K., 1992, Corrections for near surface effects; decomposition of the magnetotelluric impedance tensor and scaling corrections for regional resistivities: A tutorial: Survey in Geophysics, **13,** 341-379.

Groom, R. W., Kurtz, R. D., Jones, A. G. and Boerner, D. E., 1993, A quantitative methodology to extract regional magnetotelluric impedances and to determine the dimension of the conductivity structure: Geophys. J. Int., **115,** 1095-1118.

Hohmann, G. W., 1975, Three-dimensional induced polarisation and electromagnetic modeling: Geophysics, **40,** 309-324.

Li, Y., Yu, P., Zhang, L., Wang, J., and Wu, J., 2010, An Improved Approach On Distortion Decomposition of Magnetotelluric Impedance Tensor: 2010 SEG Annual Meeting, 17-22 October, Denver, Colorado, SEG-2010-0824.

Lilley, F. E. M., 1995, Strike direction: obtained from basic models for 3D magnetotelluric data: Three-dimensional Electromagnetics (Eds. M Oristaglio and B. Spies), 359-370. Ridgefield, Conn. USA.

Lilley, F. E. M., 1998, Magnetotelluric tensor decomposition: Part I. Theory for a basic procedure: Geophysics, **63(6)**, 1885–1897.

Lilley, F. E. M., 2012, Magnetotelluric tensor decomposition: Insights from linear algebra and Mohr diagrams: In: New achievements in geoscience (Ed: Hwee-Sam Lim) doi: 10.5772/2066.href=''http://www.intechopen.com/books/new-achievements-in-geoscience".

Lilley, F. E. M., and Weaver, J. T., 2010, Phases greater than 90° in MT data, analysis using dimensionality tools: J. Appl. Geophys., **70**, 9-16.

Jiracek, G. R., 1990, Near-surface and topographic distortions in electromagnetic induction: Survey in Geophysics, **11,** 163-203.

Jiracek, G. R., Reddig, R. P. and Kojima, R. K., 1989, Application of the Rayleigh-FFT technique to magnetotelluric modelling and correction: Phys. Earth Planet. Inter., **53,** 365-375.

Jones, A. G. and Dumas, I., 1993, Electromagnetic images of a volcanic zone: Phys. Earth Planet. Inter., **81,** 289-314.

Jones, A. G. and Groom, R. W., 1993, Strike-angle determination from the magnetotelluric impedance tensor in the presence of noise and local distortion: rotate at your perril!: Geophys. J. Int., **113,** 524-534.

Kannaujiya, S. and Israil, M., 2012, Determination of Geoelectric Strike and 2D inversion of Magnetotelluric Data from Himalayan Region: 9th Biennial International Conference and Exposition on Petroleum Geophysics, P-008, Hyderabad, India.

Kaufman, A. A., 1988, Reduction of the geological noise in magnetotelluric soundings: Geoexploration, **25,** 145-161.

Larsen, J. C., 1977, Removal of local surface conductivity effects from low frequency mantle response curves: Acta Geodaet. Geophys. et Montanist. Acad. Sci. Hung., **12,** 183-186.

LaTorraca, G. A., Madden, R. T. and Korringa, J., 1986, An analysis of the magnetotelluric impedance for three-dimensional conductivity structures: Geophysics, **51,** 1819-1829.

LeMouel, J. L. and Menvielle, 1982, Geomagnetic variation anomalies and deflection of telluric currents: Geophys. J. Roy. astr. Soc., **68,** 575-587.

McNeice, G. W. and Jones, A. G., 2001, Multisite, multifrequency tensor decomposition of magnetotelluric data: Geophysics, **66,** 158–173.

Moradzadeh, A., 1998, Electrical imaging of the Adelaide Geosyncline using magnetotellurics (MT): Ph.D. Thesis, Flinders Univ. of South Australia.

Moradzadeh, A. and White, A., 2005, An assessment of the geoelectric dimensionality of subsurface structures using magnetotelluric data: J. Sci. & Tech., Shahrood University of Technology, **6,** 59-65.

Moradzadeh, A., 2003, Static shift appraisal and its correction in magnetotelluric (MT) surveys: The 21st symposium on geosciences. 197-201, Tehran, Iran.

Pellerin, L., 1988, Use of Transient Electromagnetic Soundings to correct static shifts in Magnetotelluric data: MSc. Thesis, Univ. Utah.

Smith, J. T., 1995, Understanding telluric distortion matrices: Geophys. J. Int., **122**, 219–226.

Swift, C. M., Jr., 1967, A magnetotelluric investigation of an electrical conductivity anomaly in the southwestern of United States: Ph.D. Thesis, Mass. Inst. Tech.

Vozoff, K., 1991, The magnetotelluric method. In: Nabighian, M. N. (Ed), Electromagnetic Methods In Applied Geophysics. Society of Exploration Geophysicists, 641-712.

Wannamaker, P. E., Hohmann, G., W. and

Ward, S. H., 1984, Magnetotelluric responses of three-dimensional bodies in layered earths: Geophysics, **49,** 1517-1533.

Ward, S. H., 1967, Electromagnetic Theory for Geophysical Application, Mining Geophysics: Society of Exploration Geophysicists, 10-196.

Yee, E. and Paulson, K. V., 1987, The Canonical decomposition and its relationship to other forms of magnetotelluric impedance tensor analysis: Geophysics, **61,** 173-189.

Zhdanov, M. S., 1987, Application of space analysis of electromagnetic fields to investigation of the geoelectrical structure of the earth: Phys. App. Geophys., **125,** 483-497.

Zhang, P., Roberts, R. G. and Pedersen, L. B., 1987, Magnetotelluric strike rules: Geophysics, **52,** 267-278.